3-13-2020

Testing the Hypothesis of Compact-binary-coalescence Origin of Fast Radio Bursts Using a Multimessenger Approach

Sarah York
University of Nevada, Las Vegas, sarah.york@unlv.edu

Rea Lavi
Israel Institute of Technology

Yehudit Judy Dori
Israel Institute of Technology

MaryKay Orgill
University of Nevada, Las Vegas, marykay.orgill@unlv.edu

Repository Citation

York, S., Lavi, R., Dori, Y. J., Orgill, M. (2020). Testing the Hypothesis of Compact-binary-coalescence Origin of Fast Radio Bursts Using a Multimessenger Approach. *Journal of Chemical Education, 96*(12), 2742-2751.
http://dx.doi.org/10.1021/acs.jchemed.9b00261

The Astrophysical Journal Letters, 891:L39 (7pp), 2020 March 10 https://doi.org/10.3847/2041-8213/ab7a1b

Testing the Hypothesis of a Compact-binary-coalescence Origin of Fast Radio Bursts Using a Multimessenger Approach

Min-Hao Wang[1], Shun-Ke Ai[2], Zheng-Xiang Li[1], Nan Xing[1], He Gao[1], and Bing Zhang[2]
[1] Department of Astronomy, Beijing Normal University, Beijing 100875, People's Republic of China; gaohe@bnu.edu.cn
[2] Department of Physics and Astronomy, University of Nevada Las Vegas, NV 89154, USA
Received 2020 January 23; revised 2020 February 18; accepted 2020 February 25; published 2020 March 13

Abstract

In the literature, compact binary coalescences (CBCs) have been proposed as one of the main scenarios to explain the origin of some non-repeating fast radio bursts (FRBs). The large discrepancy between the FRB and CBC event rate densities suggests that their associations, if any, should only apply at most for a small fraction of FRBs. Through a Bayesian estimation method, we show how a statistical analysis of the coincident associations of FRBs with CBC gravitational wave (GW) events may test the hypothesis of these associations. We show that during the operation period of the advanced Laser Interferometer Gravitational-Wave Observatory (aLIGO), the detection of ∼100 (∼1000) GW-less FRBs with dispersion measure (DM) values smaller than 500 pc cm^{-3} could reach the constraint that less than 10% (or 1%) FRBs are related to binary black hole (BBH) mergers. The same number of FRBs with DM values smaller than 100 pc cm^{-3} is required to reach the same constraint for binary neutron star (BNS) mergers. With the upgrade of GW detectors, the same constraints for BBH and BNS mergers can be reached with fewer FRBs or looser requirements for the DM values. It is also possible to pose constraints on the fraction of each type of CBCs that are able to produce observable FRBs based on the event density of FRBs and CBCs. This would further constrain the dimensionless charge of black holes (BHs) in binary BH systems.

Unified Astronomy Thesaurus concepts: Radio transient sources (2008); Compact binary stars (283)

1. Introduction

Fast radio bursts (FRBs) are bright, milliseconds-duration radio transients with high dispersion measures, typically with an isotropic energy in the radio band as high as 10^{38}–10^{40} ergs (Lorimer et al. 2007; Thornton et al. 2013). The event rate density of FRBs is about 10^3 to 10^4 Gpc^{-3} yr^{-1} depending on the minimum fluence of the detected FRBs (Cordes & Chatterjee 2019; Petroff et al. 2019).

Even though a growing population of FRBs are found to repeat (Spitler et al. 2016; CHIME/FRB Collaboration et al. 2019), the majority of FRBs detected so far are apparently non-repeating. It is possible that a small fraction of FRBs are genuinely non-repeating, which may be associated with catastrophic events.

Many different models have been proposed to explain FRBs, such as binary neutron star (BNS) mergers (Totani 2013; Wang et al. 2016; Dokuchaev & Eroshenko 2017; Yamasaki et al. 2018), binary white-dwarf mergers (Kashiyama et al. 2013), mergers of charged black holes (BHs; Liu et al. 2016; Zhang 2016), collapses of supramassive rotating neutron stars (Falcke & Rezzolla 2014; Ravi & Lasky 2014; Zhang 2014; Punsly & Bini 2016), magnetar flares (Popov & Postnov 2010; Kulkarni et al. 2014; Lyubarsky 2014), BH batteries (Mingarelli et al. 2015), collisions and interactions between neutron stars and small objects (Mottez & Zarka 2014; Geng & Huang 2015; Dai et al. 2016; Huang & Geng 2016; Smallwood et al. 2019), quark novae (Shand et al. 2016), giant pulses of pulsars (Connor et al. 2016; Cordes & Wasserman 2016), cosmic combs (Zhang 2017, 2018), and superconducting cosmic strings (Yu et al. 2014). See Platts et al. (2018) for a review of the available theoretical models.

A good fraction of these models are related to compact binary coalescences (CBCs), including BNS mergers, binary black hole (BBH) mergers and black hole–neutron star (BH–NS) mergers. For BNS mergers, there have been several proposals. Totani (2013) suggested that synchronization of the magnetosphere of the two NSs shortly after the merger can power bright coherent radio emission in a manner similar to radio pulsars. Zhang (2014) suggested that if the BNS merger product is a supramassive NS (Dai et al. 2006; Zhang 2013; Gao et al. 2016), an FRB can be produced as the supramassive NS collapses into a BH as the magnetic "hair" of the BH is ejected (Falcke & Rezzolla 2014). Wang et al. (2016) proposed that during the final inspiral phase, an electromotive force would be induced on one NS to accelerate electrons to an ultra-relativistic speed instantaneously, thus generating FRB signals via coherent curvature radiation from these electrons moving along magnetic field lines in the magnetosphere of the other NS. So, theoretically, an FRB can accompany a BNS merger event right before (Wang et al. 2016), during (Totani 2013), or hundreds of seconds after (Ravi & Lasky 2014; Zhang 2014) the merger. For BBH and plunging BH–NS (mass ratio less than 0.2; Shibata et al. 2009) mergers, one would not expect bright electromagnetic counterparts for CBCs. However, if at least one of the members is charged, both dipole electric radiation and dipole magnetic radiation would be emitted from the system during the inspiral phase. The emission powers increase sharply at the final phase of the coalescence (Zhang 2016, 2019; Deng et al. 2018; Dai 2019). This would produce a brief electromagnetic signal, which may manifest itself as an FRB if coherent radio emission can be produced from the global magnetosphere of the system (Zhang 2016, 2019).

The host galaxy information is helpful to constrain the origin of FRBs. The first repeating FRB 121102 was localized in a dwarf galaxy with a redshift of 0.19273 (Scholz et al. 2016; Spitler et al. 2016; Chatterjee et al. 2017; Marcote et al. 2017; Tendulkar et al. 2017). Most recently, two non-repeating FRBs were precisely localized (FRB 180924, Bannister et al. 2019; FRB 190523, Ravi et al. 2019). Interestingly, unlike FRB 121102, the host galaxies of the latter two apparently non-repeating FRBs have a relatively low star formation rate. The locations of the FRBs have a relatively large spatial offset with

respect to the host galaxy (Bannister et al. 2019; Ravi et al. 2019). These properties are similar to those of short GRBs believed to be produced by neutron star mergers (Berger et al. 2013). These discoveries therefore revive the possibility that a fraction of FRBs might be related to BNS or neutron star–black hole (NS–BH) mergers. Because the FRB event rate density is much higher than those of CBCs and a good fraction of FRBs repeat, the CBC-associated FRBs, if they exist, should only comprise of a small fraction of the full FRB population.

CBCs are the sources of gravitational waves (GWs). A direct proof of the CBC-related FRBs would be the direct observation of FRB—CBC associations. To date, no such associations have been found. The non-detection could be discussed in two different contents. If a CBC is detected without an associated FRB counterpart, one may not draw firm conclusions regarding the non-associations. This is because current radio telescopes that detect FRBs do not cover the all-sky, so that one cannot rule out the existence of an associated FRB with the CBC. Even if the entire CBC error box was by chance covered by radio telescopes, one cannot rule out the association as a putative FRB might be beamed away from Earth. On the other hand, if an FRB is detected without an associated GW signal, the constraints on the association would be much more straightforward. First, the FRB source may be outside the GW detection horizons. If one only focuses on those FRBs that are within the horizons of GW detectors, the non-detection of an association only has one possible reason: the FRB is not from a CBC. By observing many such FRBs, one would be able to constrain the fraction f of CBC-origin FRBs.

In this Letter we develop a Bayesian model to estimate the fraction f based on the joint (non)-detection of FRBs and GWs. We claim that even for GW-less FRBs (FRBs without detected GW counterparts), an accumulation of the sample can place a constraint on f. Furthermore, based on the event rates of FRBs and BBH mergers, one may also constrain the charge of the BHs in the BBH and/or NS–BH systems.

2. Methods

2.1. Bayesian Estimation Model

Suppose that during the all-sky monitoring of CBC events by GW detectors a sample of FRBs are detected, which could be denoted as $D = (D_1, D_2, \ldots, D_N)$, where N is the total number of the FRBs in the sample. One can define $D_i = (d_i, \mathrm{DM}_i)$, where DM_i is the dispersion measure (DM) value for the ith FRB, and d_i represents whether the ith FRB is detected ($d_i = 1$) by the GW detectors or it is not ($d_i = 0$). Three components should be considered for DM estimation, of which only the intergalactic medium (IGM) should depend upon the cosmological distance. Aside from the IGM component, contributions from the Milky Way (MW) and the FRB host galaxy (host) also need to be considered.

Since $\mathrm{DM_{MW}}$ and $\mathrm{DM_{host}}$ can be only roughly modeled by simple distributions, one particular z may correspond to a wide distribution of possible DM values. In other words, a particular DM value may correspond to a wide distribution of z. We use Pi to represent the probability of the ith FRB being within the detection horizon of the GW detectors (z_h, in terms of redshift). If the redshift of the ith FRB (z_i) can be determined, it is relatively easy to get $Pi = 1$ (when $z_i < z_h$) or $Pi = 0$ (when $z_i > z_h$).

A Bayesian formula can be used to estimate the probability distribution of f as

$$\pi(f|D) = \frac{L(D; f)\pi(f)}{\int L(D; f)\pi(f)df}, \tag{1}$$

where $\pi(f)$ is the prior distribution for f and $L(D; f)$ represents the likelihood function for observing $D = (D_1, D_2, \ldots, D_N)$ sample under the hypothesis that a fraction f of the FRBs come from a specific kind of CBC events. Here we have

$$\begin{aligned} L(D; f) &= C_N^m \prod L(D_i; f) \\ &= C_N^m \prod [d_i f P_i + (1 - d_i)(1 - f P_i)], \end{aligned} \tag{2}$$

where m is the number of FRBs with GW detections for CBCs, and N is the total number of FRBs.

One can apply this model to constrain FRBs from any kind of CBC event. Ignoring the uncertainty of DM models, only the horizon z_h influences the final results, which is determined by both the CBC types and GW detectors.

2.2. DM Models and Samples

To be specific, the observed DM value can be expressed as

$$\mathrm{DM_{obs}} = \mathrm{DM_{MW}} + \mathrm{DM_{IGM}} + \mathrm{DM_{host}}. \tag{3}$$

$\mathrm{DM_{IGM}}$ depends on the cosmological distance scale and the fraction of ionized electrons in hydrogen (H, $\chi_{\mathrm{e,H}}(z)$) and helium (He, $\chi_{\mathrm{e,He}}(z)$) along the path. The latter two elements are closely related to the present-day baryon density parameter Ω_b and the fraction of baryons in the IGM, f_IGM. If both hydrogen and helium are fully ionized (valid below $z \sim 3$), the average value (for an individual line of sight; the value may deviate from this due to large-scale density fluctuations; Mcquinn 2014) can be written as (Gao et al. 2014)

$$\mathrm{DM_{IGM}}(z) = \frac{21 c H_0 \Omega_b f_\mathrm{IGM}}{64\pi G m_\mathrm{p}} \int_0^z \frac{(1 + z')dz'}{E(z')}. \tag{4}$$

The uncertainty of $\mathrm{DM_{IGM}}$ is important but complicated because of the density fluctuation of the large-scale structure. According to Mcquinn (2014), the standard deviation from the mean DM is dependent upon the profile models characterizing the inhomogeneity of the baryon matter in the IGM. Here, we use numerical simulation results of Mcquinn (2014) and Faucher-Giguère et al. (2011; purple dotted line in the bottom panel of Figure 1 in Mcquinn 2014) to account for the standard deviation.

Here, DM contribution from the MW is derived by modeling the electron density distribution in a spiral galaxy with the NE2001 model and considering a uniform spatial distribution of FRBs (Cordes & Lazio 2002; Xu & Han 2015). The value of $\mathrm{DM_{host}}$ and its uncertainty σ_host are intractable parameters as they are poorly known and related to many factors such as the local near-source plasma environment, the site of FRB in the host, the inclination angle of the galaxy disk, and the type of host galaxy (e.g., Xu & Han 2015; Luo et al. 2018). In our analysis, we assume that the type of host galaxy is similar to the MW. Moreover, an additional contribution from the local nearby plasma also should be taken into account. Here, we use $\mathrm{DM_{host}}$ to denote the total contribution from both the host galaxy and the local nearby environment. For an FRB at redshift z, the rest-frame

DM_{host} relates to the contribution to the observed DM via a factor $1+z$, i.e., $DM_{host} = DM_{host,loc}/(1+z)$.

With all three budgets in Equation (3) addressed, we generate a sample containing $\sim 10^6$ (10^7) FRBs with the redshift uniformly distributed in $z = 0$–1 (0–9). In our simulation, we assume $f_{IGM} = 0.83$ and a Planck Collaboration et al. (2018) cosmology with $\Omega_m = 0.3153$, $\Omega_b h^2 = 0.0224$, and $h = H_0/100\ \mathrm{km\ s^{-1}\ Mpc^{-1}} = 0.6736$. Based on our simulated sample, $_{Pi}$ could be estimated for any given DM_i and z_h.

3. Constraining the Fraction of FRBs from CBCs

To constrain the fraction of FRBs from different kinds of CBC events, the horizon of the GW detector is a key parameter. In principle, the GW horizon of each kind of CBC event is a function of the mass of the system. Here we choose some characteristic masses for different types of CBCs as an example.

For NS–NS mergers, the horizon is ~220 Mpc ($z_h \approx 0.05$) for aLIGO (Abramovici et al. 1992), 480 Mpc ($z_h \approx 0.1$) for aLIGO A + (LIGO Scientific Collaboration 2016), and ~2.3 Gpc ($z_h \approx 0.5$) for the proposed third-generation GW detector Einstein Telescope (ET; Punturo et al. 2010). For BH–BH mergers with a total mass of $\sim 60\,M_\odot$ ($30\,M_\odot + 30\,M_\odot$), the horizon is ~1.6 Gpc ($z_h \approx 0.3$) for aLIGO, 2.5 Gpc ($z_h \approx 0.45$) for aLIGO A+, and ~354 Gpc ($z_h \approx 40$) for ET (LIGO Scientific Collaboration 2019).

For a specific GW detector, our proposed Bayesian estimation model can be used to calculate the posterior probability density distribution of f for a given FRB sample $D = (D_1, D_2, \ldots, D_N)$ that may be detected in the future. As an example, here we focus on the accumulation of negative joint detection cases, which means that a large sample of FRBs are detected during the GW detector operation but have no joint GW signals detected, so that $m = 0$ and $d_{i=1\ldots N} = 0$. For simplicity, we assign a characteristic DM value for the whole sample, namely $DM_{i=1\ldots N} = \overline{\mathrm{DM}}$. Since only a small fraction of FRBs are expected to be well localized, which is at least true in the near future, here we assume that not all z_i could be well determined and all the Pi's are estimated with the Monte Carlo simulation method. Similarly, $P_{i=1\ldots N} = \overline{P}$ is assumed. As shown in Figure 1, $\overline{P}$ decreases from 1 to 0 with the increase of $\overline{\mathrm{DM}}$, because FRBs with smaller DM values are more likely to be within the horizon of GW detectors. Based on such a mock observational FRB sample, $\overline{P}$ can be calculated, as well as the posterior probability density distribution of f. The results are shown in Figure 1. Note that we have taken the prior distribution of f as a uniform distribution.

Since to date no detected FRBs are accompanied by GW triggers, the posterior probability density distribution of f peaks at $f = 0$. Given the value of $\overline{\mathrm{DM}}$ and z_h, the posterior probability density distribution of f would become narrower as the sample accumulates, whereas given the sample size N, the distribution would become narrower as $\overline{\mathrm{DM}}$ decreases or z_h increases. Here we define $\overline{f}$ as the upper limit of the fraction of FRBs associated with a specific type of CBC, where the probability of $f < \overline{f}$ is larger than 99.7% (equivalent 3σ confidence level). In Figure 2 and Table 1, we show how $\overline{f}$ evolves as the sample accumulates for different $\overline{\mathrm{DM}}$ values and different GW detectors.

It is obvious that when FRBs with small $\overline{\mathrm{DM}}$ values are considered (all of the FRB sources are within the horizon of GW detectors) only a small number of FRB detections without GW counterparts can lead to a low level of $\overline{f}$. This is shown by the black lines in Figure 2. To be specific, ~10 FRBs without GWs

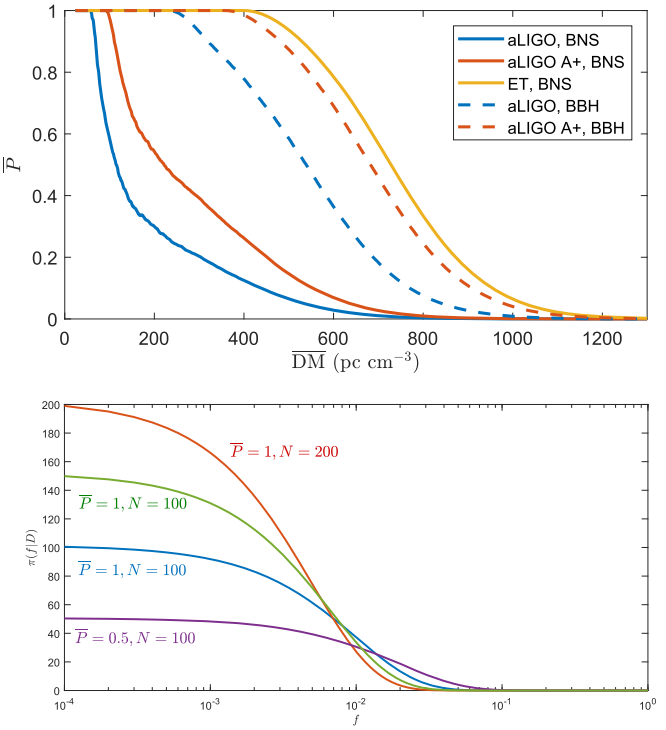

Figure 1. The top panel shows the possibility $\bar{P}$ of FRBs with given DM values located within the horizon of different GW detectors. The solid lines are for BNS cases and the dashed lines are for BBH cases. Lines with different colors refer to different GW detectors. The bottom panel shows the posterior distribution of the fraction f after N FRBs with the same DM value (so is the $\bar{P}$ value) being detected. Lines with different colors correspond to different values of N and $\bar{P}$.

can constrain $\overline{f}$ below 50%; ~55 FRBs without GWs can constrain $\overline{f}$ below 10%; and ~590 FRBs can constrain $\overline{f}$ below 1%.

As shown in Table 1, for a certain GW detector toward a specific type of CBC, the increase of $\overline{\mathrm{DM}}$ leads to looser constraints. In other words, more detections are required to obtain the same constraint on $\overline{f}$. However, for different GW detectors, to reach the same constraint level with the same number of detections, the required $\overline{\mathrm{DM}}$ is totally dependent on the horizon of the GW detectors.

From GW observations, the event rate density of BBH mergers and BNS mergers are estimated as (Abbott et al. 2019, 2020)

$$\dot{\rho}_{\mathrm{BBH}} \sim 53.2^{+58.5}_{-28.8}\ \mathrm{Gpc^{-3}\ yr^{-1}}, \tag{5}$$

with a 90% confidence level and

$$\dot{\rho}_{\mathrm{BNS}} \sim 250 - 2810\ \mathrm{Gpc^{-3}\ yr^{-1}}, \tag{6}$$

which is obviously lower than that of FRBs, which could be estimated as[3] (Zhang 2016)

$$\dot{\rho}_{\mathrm{FRB}} \sim (5.7 \times 10^3\ \mathrm{Gpc^{-3}\ yr^{-1}}) \times \left(\frac{D_z}{3.4\ \mathrm{Gpc}}\right)^{-3} \left(\frac{\dot{N}_{\mathrm{FRB}}}{2500}\right). \tag{7}$$

[3] This estimation is good for FRBs with a luminosity that is larger than 10^{43} ergs^{-1}. If a significant fraction of FRBs have a lower luminosity, the FRB event rate could be even larger. In this case, the maximum possible value of $\overline{f}_{\mathrm{BBH}}$ and $\overline{f}_{\mathrm{BNS}}$ would be even smaller, so that more GW-less FRBs are needed to achieve meaningful constraints with our proposed method.

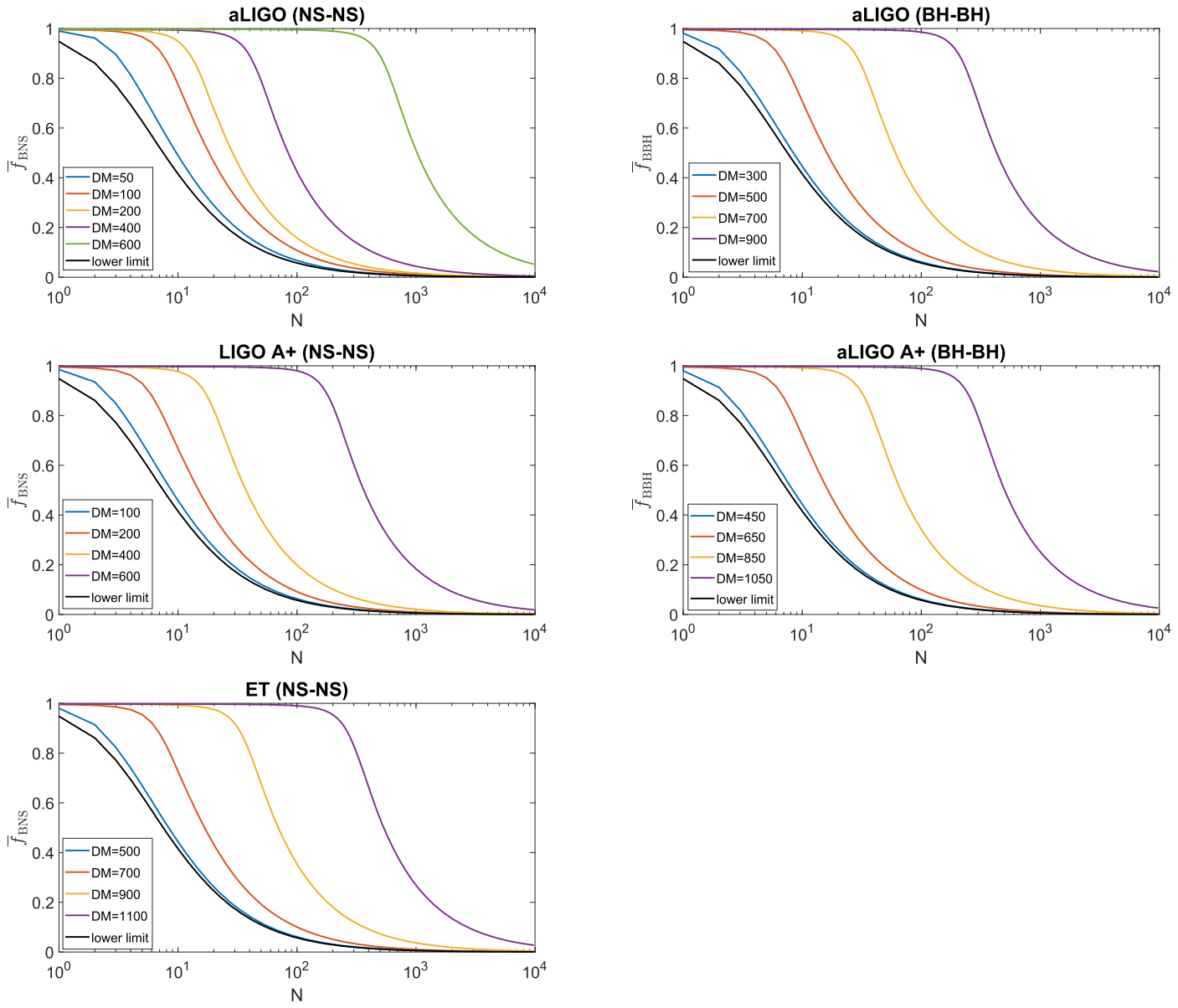

Figure 2. Constraints on $\overline{f}$ as the FRB sample with different $\overline{\rm DM}$ values accumulates for various GW detector operations. The left panel represents the constraints from FRBs and GW observations of a BNS merger. The right panel represents the constraints from FRBs and GW observations of a BBH merger. The black line in each figure stands for the case where FRB sources are within the horizon of GW detector.

Here the all-sky FRB rate $\dot{N}_{\rm FRB}$ is normalized to 2500 $\rm d^{-1}$ (Keane & Petroff 2015), and the comoving distance D_z is normalized to $z = 1$. The ratio between the rates of different kinds of CBCs and the event rate of FRBs provides the maximum possible value of $\overline{f}$. Based on current results, we have $\overline{f}_{\rm BBH} < 0.93^{+1.03}_{-0.50}\%$ (with a 90% confidence level) and $\overline{f}_{\rm BNS} < 4.39\%$–$49.3\%$. According to Table 1, we find that for aLIGO (LIGO A+), ∼1000 GW-less FRBs with $\overline{DM} < 500\ (600)$ pc $\rm cm^{-3}$ could achieve a meaningful constraint, where $\overline{f_{\rm BBH}} < 1\%$. For the third generation of the GW detector ET, almost all the sources of FRBs are within its horizon for BBH mergers, so the constraints come to the limiting case shown by the black lines in Figure 2: ∼600 FRBs with an arbitrary $\overline{\rm DM}$ value can reach the constraint that less than 1% FRBs are related to BBH mergers. Since the BNS merger rate is very uncertain, the maximum possible value of $\overline{f}_{\rm BNS}$ is also with large uncertainty. In an optimistic situation ($\overline{f}_{\rm BNS} < 49.3\%$), we find that for aLIGO (LIGO A+), ∼30 (15) GW-less FRBs with $\overline{DM} < 200$ pc $\rm cm^{-3}$ could achieve a meaningful constraint, where $\overline{f_{\rm BNS}} < 50\%$, and ∼1000 (400) GW-less FRBs with $\overline{DM} < 600$ pc $\rm cm^{-3}$ could reach the same constraint. For ET, ∼10 FRBs with $\overline{DM} < 500$ pc $\rm cm^{-3}$ can reach the constraint that less than 50% FRBs are related to BNS mergers. On the other hand, in a pessimistic situation ($\overline{f}_{\rm BNS} < 4.39\%$), we find that for aLIGO (LIGO A+), ∼400 (200) GW-less FRBs with $\overline{DM} < 200$ pc $\rm cm^{-3}$ could achieve a meaningful constraint, where $\overline{f_{\rm BNS}} < 5\%$, and ∼1000 (500) GW-less FRBs with $\overline{DM} < 400$ pc $\rm cm^{-3}$ could reach the same constraint. For ET, ∼140 FRBs with $\overline{DM} < 500$ pc $\rm cm^{-3}$ can reach the constraint that less than 5% FRBs are related to BNS mergers. It is interesting to note that, in this case, for a similar $\overline{\rm DM}$ value and a

Table 1
Constraints on $\overline{f}$ for FRB Samples

	aLIGO			LIGO *A*+			ET		
	$\overline{\mathrm{DM}}$	$\overline{f}_{\mathrm{BNS}}$	N	$\overline{\mathrm{DM}}$	$\overline{f}_{\mathrm{BNS}}$	N	$\overline{\mathrm{DM}}$	$\overline{f}_{\mathrm{BNS}}$	N
NS–NS	50	50%	10	100	50%	9	500	50%	9
	50	10%	65	100	10%	62	500	10%	59
	50	5%	135	100	5%	127	500	5%	122
	50	1%	692	100	1%	648	500	1%	628
	100	50%	18	200	50%	15	700	50%	17
	100	10%	108	200	10%	91	700	10%	100
	100	5%	220	200	5%	186	700	5%	204
	100	1.1%	1000	200	1%	946	700	1%	1000
	200	50%	29	400	50%	37	900	50%	70
	200	10%	160	400	10%	202	900	10%	364
	200	5%	325	400	5%	409	900	5%	733
	200	1.6%	1000	400	2.1%	1000	900	3.7%	1000
	400	50%	84	600	50%	364	1100	50%	535
	400	10%	438	600	18%	1000	1100	27%	1000
	400	5%	880						
	600	51%	1000						
	$\overline{\mathrm{DM}}$	$\overline{f}_{\mathrm{BBH}}$	N	$\overline{\mathrm{DM}}$	$\overline{f}_{\mathrm{BBH}}$	N	$\overline{\mathrm{DM}}$	$\overline{f}_{\mathrm{BBH}}$	N
BH–BH	300	50%	9	450	50%	8	⋯	50%	8
	300	10%	60	450	10%	59	⋯	10%	55
	300	1%	631	450	1%	627	⋯	1%	590
	500	50%	16	650	50%	16			
	500	10%	97	650	10%	99			
	500	1%	1000	650	1%	1000			
	700	50%	61	850	50%	67			
	700	10%	319	850	10%	352			
	700	3.2%	1000	850	1%	3556			
	900	50%	431	1050	50%	502			
	900	10%	2193	1050	10%	2518			
	900	2.2%	10000	1050	2.5%	10000			

same GW detector, the required sample size of FRBs required in order to achieve meaningful constraints is comparable between BNSs and BBHs.

Note that here we only show results for BNS and BBH mergers, as the constraints for the NS–BH merger model should be similar to the BNS merger case, except that the horizon of GW detectors for NS–BH mergers is slightly larger than that of BNS mergers, which leads to a more stringent constraint on $\overline{f}_{\mathrm{NS--BH}}$ with the same DM values and number of detections. The example that we show here is based on a simplified situation where a characteristic DM value is assigned for the entire FRB sample, and all FRBs in the sample are neither well localized nor associated with a GW detection. The results could be used as a reference for more realistic cases. For instance, if we have an FRB sample with a characteristic DM value as the maximum of the whole sample, namely $DM_{i=1\ldots N} \leqslant \overline{\mathrm{DM}}$, in order to achieve a similar constraint on $\overline{f}$, fewer FRBs are required, i.e., N value in Table 1 would become much smaller. On the other hand, if precise positioning is achieved for some FRBs in the sample, and if their distances are determined within the detection horizon of the monitoring GW detectors but there is no GW detection, these sources will increase their weight so that fewer samples are needed to obtain the same constraint on $\overline{f}$. Finally, if some FRBs in the sample are associated with GW signals and the signals are from one kind of CBC event, then the distribution center value of f for this CBC-origin FRB model is no longer 0, but the upper limit of the proportion could still be limited with the accumulation of FRBs in the sample.

4. Constraints on BH Charge

A number of FRB models based on BNS mergers have been proposed. These models invoke different BNS merger physics, so it is not easy to constrain NS properties through negative joint detection between FRBs and BNS merger GW events. On the other hand, the FRB model based on BBH mergers directly depends on the amount of dimensionless charge carried by the BHs with essentially no dependence on other parameters (Zhang 2016, 2019). Consequently, the accumulation of FRBs without BBH merger associations can place interesting constraints on the amount of charge carried by BHs.

According to Zhang (2016), an FRB may be made from BBH mergers when at least one of the BHs carries a dimensionless charge $\hat{q} \equiv Q/Q_c > 10^{-9}$–$10^{-8}$, where $Q_c = 2\sqrt{G}M = (1.0 \times 10^{31}\mathrm{e.s.u.})(M/10\,M_\odot)$. Assuming that the radio efficiency of a charged CBC luminosity is η_r and that there is equal mass in the BBH system, the FRB luminosity can be estimated as (Zhang 2019)

$$L_{\mathrm{FRB}} = \frac{1}{6}\frac{c^5}{G}\hat{q}^2\eta_r\left(\frac{r_s}{a}\right)^{-4} = \frac{1}{96}\frac{c^5}{G}\hat{q}^2\eta_r$$
$$= (3.8 \times 10^{57}\ \mathrm{erg\ s^{-1}})\ \xi^2, \quad (8)$$

where

$$\xi \equiv \hat{q}\sqrt{\eta_r}, \tag{9}$$

$r_s = 2GM/c^2$ is the Schwarzschild radius of each BH and $r_s/a = 1/2$ at the merger.

For a sample of GW-less FRB detection, where the minimum FRB luminosity within the sample is $L_{\rm min}$, one can define a critical value for the combination of BH charge and radio efficiency, ξ_c, where

$$(3.8 \times 10^{57}\ {\rm erg\ s^{-1}})\ \xi_c^2 = L_{\rm min}, \tag{10}$$

namely

$$\xi_c^2 = 2.6 \times 10^{-17} L_{\rm min,41}, \tag{11}$$

or

$$\xi_c = 5.1 \times 10^{-9} L_{\rm min,41}^{1/2}. \tag{12}$$

Note that the FRBs produced by charged BBH mergers are essentially isotropic. If all BBH systems are charged, and a good fraction of BBH systems satisfy $\xi > \xi_c$, with sufficient FRB sample size, there should be some FRBs together with the GW counterparts detected. Otherwise, we can put an upper limit to the fraction of BBH systems with $\xi > \xi_c$, which could be estimated as

$$F_{\xi>\xi_c} = \frac{\dot{\rho}_{\rm FRB}}{\dot{\rho}_{\rm BBH}} \times \overline{f}_{\rm BBH} \sim 1.0^{+1.1}_{-0.5} \times \left(\frac{D_z}{3.4\ {\rm Gpc}}\right)^{-3} \left(\frac{\dot{N}_{\rm FRB}}{2500}\right) \times \left(\frac{f_{\rm BBH}}{0.93\%}\right). \tag{13}$$

Here, we normalize $\overline{f}_{\rm BBH}$ to 0.93%, which is the maximum possible value of $\overline{f}_{\rm BBH}$ according to current observations. Obviously, a more stringent constraint on $\overline{f}_{\rm BBH}$ leads to a more meaningful constraint on $F_{\xi>\xi_c}$.

5. Conclusion and Discussion

Many models have been proposed to explain the origin of FRBs. Among them, several CBC-origin models have been discussed to interpret non-repeating FRBs. Since CBCs are main targets for GW detectors, it is possible to combine the joint FRB and GW data to test these hypotheses. Since the event rate density of FRBs is much greater than the event rate density of CBCs, it is believed that at most only a small portion of FRBs could originate from CBCs. The continuous observational campaigns in both the GW field and the FRB field makes it possible to achieve FRB–GW joint detections if such associations are indeed naturally occurring. A sufficient number of the non-detections of GW sources from FRBs can also place interesting constraints on these scenarios. We developed a Bayesian estimation method to constrain the fraction f of CBC-origin FRBs using the future joint GW and FRB observational data.

The size of the FRB sample needed to make a sufficient constraint depends on the GW detection horizon for the particular type of CBC and the DM values of the observed FRBs. According to the published FRB sample, the mean value of DM distribution is approximately 668.3 pc cm^{-3}, with the range of 203.1 pc cm^{-3} to 1111 pc cm^{-3} for the 1σ confidence interval and 103.5 pc cm^{-3} to 1982.8 pc cm^{-3} for the 3σ confidence interval.[4] The DM distribution of the observed FRBs is sufficient to constrain BBH merger models. For example, only ~100 GW-less FRBs with $\overline{DM} < 500$ pc cm^{-3} in the aLIGO era can reach the constraint that the fraction of FRBs from BBH mergers is less than 10%. Since the aLIGO horizon for BNS mergers is small, it would take a long time to reach the desired sample to constrain the BNS-origin FRB models. This process will speed up in the LIGO A+ and ET era.

We also proposed a method to constrain the charge of BHs in BBH merger systems. With the fraction of no-BBH-merger FRBs constrained to below $\overline{f}_{\rm BBH} < 0.93^{+1.03}_{-0.50}\%$ for relevant FRBs whose DM values fall within the BBH merger horizon, one can start to place a limit on the BH charge for the first time, as shown in Equations (12) and (13).

Different BNS-FRB models (Totani 2013; Zhang 2014; Wang et al. 2016) predict that FRBs occur in different merging phases, therefore one should search BNS–FRB associations with different time offsets. These different models also predict different degrees of beaming angles (e.g., for FRBs produced during and after the merger, only a small fraction of the solid angle is transparent for radio waves). Our constraints on the validity of these models should properly consider the beaming correction of the observed event rate of FRBs.

This work is supported by the National Natural Science Foundation of China under grant Nos. 11722324, 11690024, 11603003, 11633001, the Strategic Priority Research Program of the Chinese Academy of Sciences, grant No. XDB23040100 and the Fundamental Research Funds for the Central Universities.

ORCID iDs

He Gao https://orcid.org/0000-0002-3100-6558
Bing Zhang https://orcid.org/0000-0002-9725-2524

References

Abbott, B. P., Abbott, R., Abbott, T. D., et al. 2017, PhRvL, 119, 161101
Abbott, B. P., Abbott, R., Abbott, T. D., et al. 2019, ApJL, 882, L24
Abbott, B. P., Abbott, R., Abbott, T. D., et al. 2020, arXiv:2001.01761
Abramovici, A., Althouse, W. E., Drever, R. W. P., et al. 1992, Sci, 256, 325
Bannister, K. W., Deller, A. T., Phillips, C., et al. 2019, Sci, 365, 565
Berger, E., Leibler, C. N., Chornock, R., et al. 2013, ApJ, 779, 18
Chatterjee, S., Law, C. J., Wharton, R. S., et al. 2017, Natur, 541, 58
CHIME/FRB Collaboration, Amiri, M., Bandura, K., et al. 2019, Natur, 566, 230
Connor, L., Sievers, J., & Pen, U.-L. 2016, MNRAS, 458, L19
Cordes, J. M., & Chatterjee, S. 2019, ARA&A, 57, 417
Cordes, J. M., & Lazio, T. J. W. 2002, arXiv:astro-ph/0207156
Cordes, J. M., & Wasserman, I. 2016, MNRAS, 457, 232
Dai, Z. G. 2019, ApJL, 873, L13
Dai, Z. G., Wang, J. S., Wu, X. F., et al. 2016, ApJ, 829, 27
Dai, Z. G., Wang, X. Y., Wu, X. F., & Zhang, B. 2006, Sci, 311, 1127
Deng, C.-M., Cai, Y., Wu, X.-F., et al. 2018, PhRvD, 98, 123016
Dokuchaev, V. I., & Eroshenko, Y. N. 2017, arXiv:1701.02492
Falcke, H., & Rezzolla, L. 2014, A&A, 562, A137
Faucher-Giguère, C.-A., Kereš, D., & Ma, C.-P. 2011, MNRAS, 417, 2982
Gao, H., Li, Z., & Zhang, B. 2014, ApJ, 788, 189
Gao, H., Zhang, B., & Lü, H.-J. 2016, PhRvD, 93, 044065
Geng, J. J., & Huang, Y. F. 2015, ApJ, 809, 24
Huang, Y. F., & Geng, J. J. 2016, in ASP Conf. Ser. 502, Frontiers in Radio Astronomy and FAST Early Sciences Symposium 2015, ed. L. Qain & D. Li (San Francisco, CA: ASP), 1
Kashiyama, K., Ioka, K., & Mészáros, P. 2013, ApJL, 776, L39

[4] Here we use the data presented in the FRB catalog Petroff et al. (2016; http://www.frbcat.org.

Keane, E. F., & Petroff, E. 2015, MNRAS, 447, 2852
Kulkarni, S. R., Ofek, E. O., Neill, J. D., et al. 2014, ApJ, 797, 70
LIGO Scientific Collaboration 2016, The LSC–Virgo White Paper on Instrument Science (2016–2017 edition)
LIGO Scientific Collaboration 2019, The LSC–Virgo White Paper on Instrument Science
Liu, T., Romero, G. E., Liu, M.-L., et al. 2016, ApJ, 826, 82
Lorimer, D. R., Bailes, M., McLaughlin, M. A., et al. 2007, Sci, 318, 777
Luo, R., Lee, K., Lorimer, D. R., & Zhang, B. 2018, MNRAS, 481, 2320
Lyubarsky, Y. 2014, MNRAS, 442, L9
Marcote, B., Paragi, Z., Hessels, J. W. T., et al. 2017, ApJL, 834, L8
Mcquinn, M. 2014, ApJL, 780, L33
Mingarelli, C. M. F., Levin, J., & Lazio, T. J. W. 2015, ApJL, 814, L20
Mottez, F., & Zarka, P. 2014, A&A, 569, A86
Petroff, E., Barr, E. D., Jameson, A., et al. 2016, PASA, 33, e045
Petroff, E., Hessels, J. W. T., & Lorimer, D. R. 2019, A&ARv, 27, 4
Planck Collaboration, Aghanim, N., Akrami, Y., et al. 2018, arXiv:1807.06209
Platts, E., Weltman, A., Walters, A., et al. 2018, PhR, 821, 1
Popov, S. B., & Postnov, K. A. 2010, in Evolution of Cosmic Objects through their Physical Activity, Proceedings of the Conference Dedicated to Viktor Ambartsumian's 100th Anniversary, ed. H. A. Harutyunian, A. M. Mickaelian, & Y. Terzian (Yerevan: Gitutyun of NAS RA), 129
Punsly, B., & Bini, D. 2016, MNRAS, 459, L41
Punturo, M., Abernathy, M., Acernese, F., et al. 2010, CQGra, 27, 194002
Ravi, V., Catha, M., D'Addario, L., et al. 2019, Natur, 572, 352
Ravi, V., & Lasky, P. D. 2014, MNRAS, 441, 2433
Scholz, P., Spitler, L. G., Hessels, J. W. T., et al. 2016, ApJ, 833, 177
Shand, Z., Ouyed, A., Koning, N., et al. 2016, RAA, 16, 80
Shibata, M., Kyutoku, K., Yamamoto, T., et al. 2009, PhRvD, 79, 044030
Smallwood, J. L., Martin, R. G., & Zhang, B. 2019, MNRAS, 485, 1367
Spitler, L. G., Scholz, P., Hessels, J. W. T., et al. 2016, Natur, 531, 202
Tendulkar, S. P., Bassa, C. G., Cordes, J. M., et al. 2017, ApJL, 834, L7
Thornton, D., Stappers, B., Bailes, M., et al. 2013, Sci, 341, 53
Totani, T. 2013, PASJ, 65, L12
Wang, J.-S., Yang, Y.-P., Wu, X.-F., et al. 2016, ApJL, 822, L7
Xu, J., & Han, J. L. 2015, RAA, 15, 1629
Yamasaki, S., Totani, T., & Kiuchi, K. 2018, PASJ, 70, 39
Yu, Y.-W., Cheng, K.-S., Shiu, G., et al. 2014, JCAP, 11, 040
Zhang, B. 2013, ApJ, 763, L22
Zhang, B. 2014, ApJL, 780, L21
Zhang, B. 2016, ApJL, 827, L31
Zhang, B. 2017, ApJL, 836, L32
Zhang, B. 2018, ApJL, 854, L21
Zhang, B. 2019, ApJL, 873, L9